DELFT UNIVERSITY OF TECHNOLOGY

REPORT 12-09

INFLUENCE OF STATOR SLOTTING ON THE PERFORMANCE OF
PERMANENT-MAGNET MACHINES WITH CONCENTRATED
WINDINGS

H. VU XUAN, D. LAHAYE, H. POLINDER AND J. A. FERREIRA

Influence of Stator Slotting on the Performance of Permanent-Magnet Machines with Concentrated Windings

Hung Vu Xuan[1], D. Lahaye[2], H. Polinder[1], J. A. Ferreira[1]

[1]Electrical Power Processing, [2]Delft Institute of Applied Mathematics
Delft University of Technology, The Netherlands

The use of slotted stator permanent-magnet machines with concentrated windings is increasing in industry. In this paper, the effect of the slot opening on flux linkage, internal voltage, mean torque, rotor eddy current loss and stator iron losses is evaluated. This gives new insight into the influence of slotting on the performance of machines with a small slot opening. In addition, the slot opening can be chosen to maximize the internal voltage and the mean torque while minimizing the total iron loss. The limitations of the traditional analytical design model with small slot openings for permanent magnet machines are reported. Carter factor expressions found in literature are evaluated by comparing them with finite-element computations. The finite element computations in turn are validated using measurements on two machines with semi-open slots and one machine with fully open slots. The measured and simulated values for amplitude and waveform of the flux linkage and internal voltages are in good agreement.

Index Terms— **Eddy current loss, permanent-magnet machine, slotting effect, fringing effect, transient FEM.**

I. INTRODUCTION

THE USE of permanent-magnet (PM) machines with concentrated windings is increasing. This is because it has advantages such as a simple and rugged structure, short end-windings, ease of manufacturing, cost-effectiveness, a high power density and torque density. With these advantages, an exterior rotor PM machine with concentrated windings is very suitable to be integrated into a flywheel of electric vehicle, wind turbine or vessel application [1], [2].

In this paper, the influence of the slotting effect on the performance of an exterior rotor PM machine with concentrated windings as shown in Fig. 1 is investigated. It is used as a power supply for the domestic load of small-scale ship application.

F.W. Carter has been the first to propose the use of an equivalent air gap to consider the slotting effect [3], [4]. The equivalent air gap is equal to the physical air gap multiplied by the so-called "Carter factor/coefficient". This concept was well accepted for design of electric machines. In [4]-[6], the authors used conformal transformations to calculate the Carter factor and/or the air gap magnetic field. The Carter factor might be calculated by analytical methods [7], [8]. In [5], [9], the relative permeance function, which can be obtained by conformal mapping, is used to account for the slotting effect on the air gap magnetic field. According to this method, the air gap flux density of the slotted stator machine is equal to the air gap flux density of slotless machine multiplied by the relative permeance function. Methods based on conformal mapping have an important drawback because it is assumed that the slot width is much smaller than its height [5], [6], [9]. In [10], the influence of the slot opening on the harmonics of the magnetomotive force of concentrated windings was investigated. In [11], [12], the authors used finite-element-method (FEM) computations to study the slotting effect on the air gap flux density.

Recently, in [13]-[15], the authors made efforts to improve the analytical model using a sub-domain method accounting for the influence of the tooth tips of surface-mounted of PM machines. In [11], Dajaku and Gerling proposed an analytical model for the case of double-side slotting. All methods based on analytical solutions including conformal transformations have a limitation, namely that they cannot consider the influence of magnetic saturation. Therefore, calculation errors might be significant for PM machines operating in deep magnetic saturation.

The first contribution of this paper is that it presents a comprehensive study about the influence of slotting effect on the magnetic field in air gap, the magnets, the flux linkage, the internal voltage, the electromagnetic torque, the rotor eddy
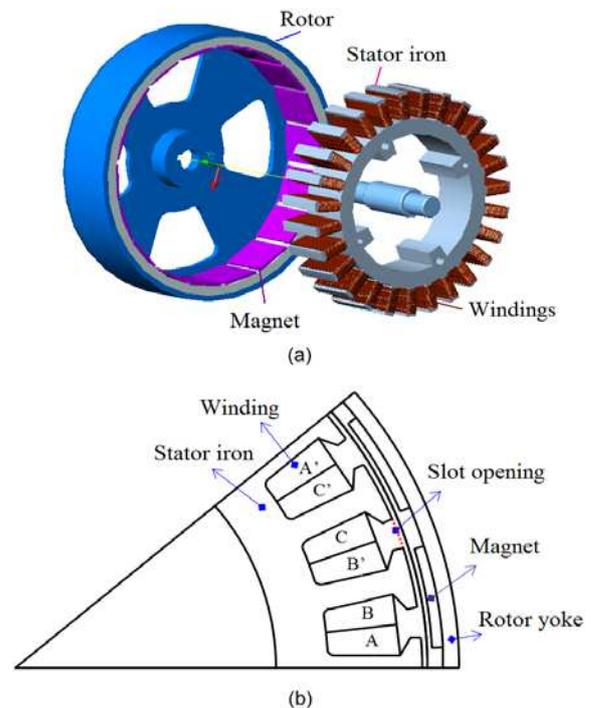

Fig. 1. Prototype of the studied concentrated winding exterior rotor surface-mounted PM machine. (a) Three-dimensional geometry. (b) Two-dimensional cross-section.

current loss, and the stator iron loss of the fractional slot PM machine with concentrated windings. Based on the analysis results, the slot opening can be chosen to reach the maximum internal voltage and mean torque. Although several authors investigated the influence of the slotting effect, most authors have focused on the influence of the slotting effect on the magnetic field in the air gap and the cogging torque [9]-[20]. The second contribution of the paper is that it indicates a limitation of the traditional literature using the Carter factor for representing the slotting effect in PM machines with small slot openings. As a result, this analysis gives insight into the influence of the slotting effect on flux linkage, internal voltage, and mean torque at small slot opening.

In this paper, nonlinear transient two-dimension FEM including rotor motion and coupling with a circuit model as well as static FEM are used for the computations [19]. FEM analysis is known as an accurate method for predicting the performance of PM machines considering effects such as slotting, fringing, and magnetic saturation. Two-dimensional FEM (2D-FEM) is accurate for calculating magnetic field, voltage, torque, and stator iron loss [19]. For calculating rotor eddy current losses, the three-dimensional transient FEM is accurate but very time-consuming. Nonlinear transient 2D-FEM including rotor motion ignores the influence of magnet ends. However, it can be used to quantify and compare the influence of the slotting effect on iron losses of PM machines considered in this study.

Three machines are used in this paper. They have a rated speed of 3150 rpm, an air gap length of 2 mm, 27 slots and 18 poles. Machine A is used in Sections II to VIII.A and has slot opening of 6 mm and tooth width of 5 mm. Machines B and C are used in Section VIII.B for additional experimental validation of the transient FEM model. They have a tooth width of 8 mm. Machine B is a semi-open slot with slot opening of 4 mm, while machine C is a fully open slot with slot opening of 13 mm. The BH curve of steels can be found in [19] and [20].

This paper is organized as follows. In Sections II to VI, the slotting effect on the magnetic field in air gap and magnets, flux linkage, internal voltage, torque, rotor eddy current loss, stator iron loss and total loss is investigated. Next, Carter factor expressions in literature are evaluated by comparing them with FEM computations in Section VII. Section VIII describes the experimental validation of slotting effect on flux linkage and internal voltage is presented in. Lastly, conclusion is drawn in Section IX.

II. INFLUENCE OF SLOT OPENING ON DISTRIBUTION OF MAGNETIC FIELD IN AIR GAP

Slotting influences the magnetic field in the air gap in two ways. Firstly, it reduces the average magnetic flux per pole. Secondly, slotting affects the distribution of the flux in the air gap, as shown in Fig. 2 and Fig. 3, [9], [15], [20]. As a result, slotting leads to a non-homogeneous air gap flux density. At the positions opposite to a slot opening with low permeability, the flux density is smaller than that at the positions opposite to tooth tips with high permeability. The non-homogeneousness

of the air gap flux density results in voltage ripple, cogging torque or torque ripple.

Fig. 2 shows calculation results of the radial flux density in the middle of the air gap for full-open slot, semi-open slot and closed slot. Clearly, the slotting effect on the flux density increases with increasing slot opening. With fully open slot, the slotting effect is greatest. The average radial flux density in the air gap reduces by about 20% of the value for closed slots, and the radial flux density waveform is highly distorted. With closed slots, the air gap flux density is homogeneous along the circumferential magnets.

The air gap flux density can be represented as a function of the radius, the stator angle (mechanical angle in the stator coordinate), and the rotor angle [1], [9], [20]. Fig. 3 illustrates the radial air gap flux density at different radii. As can be seen, when the radius increases the slotting effect reduces, but it is still significant. The air gap flux density at positions corresponding to the edge of the stator teeth has a sharp peak. This is known as the slot edge effect.
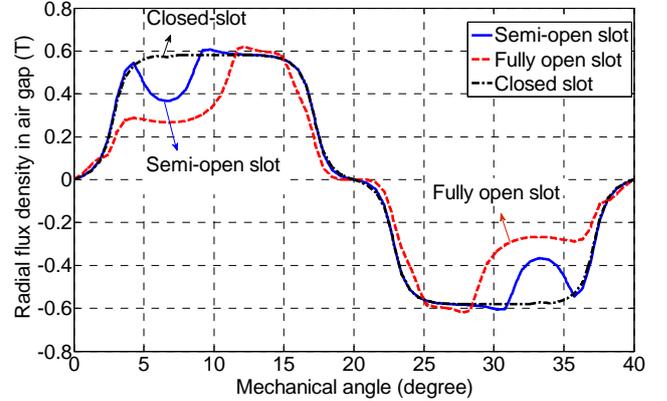

Fig. 2. Radial flux density in the middle of the air gap for full-open slot, semi-open slot and closed slot during no-load.
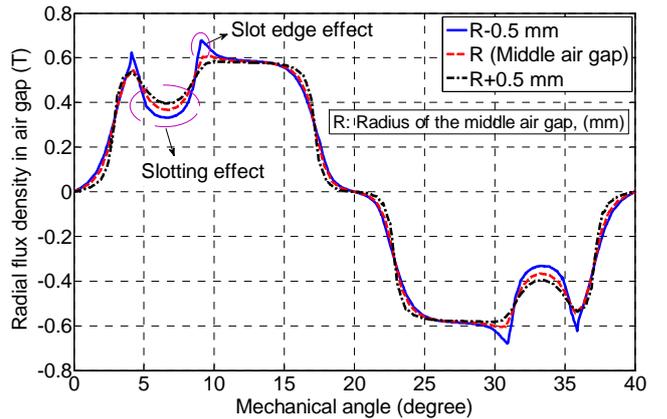

Fig. 3. Radial air gap flux density at different radii for semi-open slot during no-load.

III. INFLUENCE OF SLOT OPENING ON DISTRIBUTION OF MAGNETIC FIELD IN MAGNETS

In this section, the distribution of the flux density in the magnets is presented. Fig. 4 illustrates the radial flux density in the magnets and the air between adjacent magnets [20]. The

effects inside the magnets can be divided into the slotting effect and the magnet edge effect. It can be seen from this figure that the edge effect is negligibly small at the arc on the surface of magnet. However, for the arc in the middle of magnets, due to the effect of leakage flux at the edges of the magnets, the magnet flux density gets a peak value at the edges. For the outside of the magnet, i.e., air between adjacent magnets, the edge effect can also be explained similarly. However, the direction of the leakage flux density in the air between adjacent magnets inverts the direction of the leakage flux inside the magnet. Therefore, the flux density waveform at the magnet edges in Fig. 4 has a jumping step from positive value to negative value and inverse.

Fig. 5 shows the radial flux density in the middle of the magnets in case of semi-open slot, fully open slot, and closed slot in case of no-load. It can be seen that in a fully open slot PM machine, the magnet flux density is distorted stronger than in the semi-open slot PM machine. Therefore, the predicted eddy current loss of the fully open slot is higher than in case of semi-open slot. For the closed slot, the radial flux density inside the magnets is flat, but has a sharp peak at the edge of the magnets.

The edge effect produces a high flux density at the edge of the magnets, while the slotting effect causes variation of the flux density in the magnets. Therefore, the combination of the slotting effect and the edge effect of the magnet can be one of the reasons that lead to higher magnet eddy current loss.
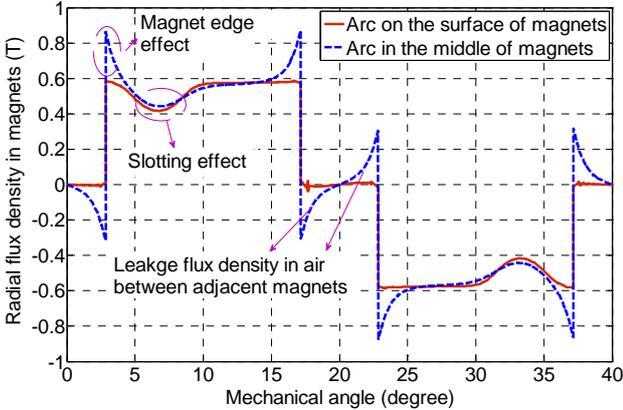

Fig. 4. Radial flux density in the magnets for semi-open slot during no-load.
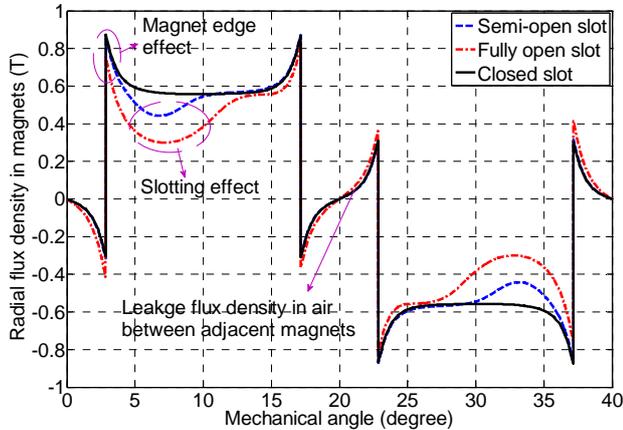

Fig. 5. Radial flux density in the magnets for full-open slot and semi-open slot during no-load.

IV. INFLUENCE OF SLOT OPENING ON FLUX LINKAGE AND INTERNAL VOLTAGE

In the previous section, the influence of the slotting effect on the magnetic field was discussed. This section presents the influence of the slotting effect on the flux linkage and the internal voltage.

The flux linkage ϕ and the internal voltage e of a turn can be calculated in two-dimensional FEM as, [19]-[23]

$$\phi = \frac{L}{S}\left(\iint_{\Omega^+} A_z d\Omega - \iint_{\Omega^-} A_z d\Omega \right) \quad (1)$$

$$e = -\frac{d\phi}{dt} \quad (2)$$

where, L is the length of stator iron, Ω^+ and Ω^- are respectively the integral areas corresponding to the go and return sides of the equivalent conductors of the stator windings, S is the cross section area of the equivalent conductors, and A_z is the magnetic vector potential in the z-direction.

Fig. 6 shows a computed flux line plot of a nearly closed slot PM machine. The relationship between the flux linkage amplitude of a turn and the slot opening is presented in Fig.7. Fig. 8 presents the relationship between the maximum internal voltage of a turn and the slot opening in no-load at a rotor speed of 3150 rpm, calculated by a transient FEM model including rotor motion. Magnetic saturation is taken into account in most calculation in this paper, except for a few cases shown in Fig. 7 and Fig. 8. The BH curve of the steel used can be found in [19], [20]. The flux linkage and the internal voltage reach a maximum value at a slot opening of around 4 mm for the case magnetic saturation is considered. With the slot opening in the range of 0 to 4 mm (this range is called the range of small slot opening) both internal voltage and flux linkage amplitudes decrease when the slot opening decreases. This is because leakage flux passing through tooth tip increases. With the slot opening greater than 4 mm, internal voltage and flux linkage amplitudes decrease when the slot opening increases. It is also shown in Fig.7 and Fig. 8 that the permeability of the stator steel strongly affects the flux linkage and the voltage amplitude. When the permeability of the stator steel increases, the flux linkage and the voltage amplitude increase. In addition, the range of small slot opening is smaller when the relative permeability of steel increases. Looking at the flux distribution in Fig. 6a, especially the leakage flux passing through the tooth tips, we see that the range of small slot opening always exists even when the ideal stator steel with infinite relative permeability is used.

Conventional analytical models based on the Carter factor on the contrary predict that the Carter factor increases with decreasing slot opening. Thus, the air gap flux density increases and internal voltage increases. Therefore, the trend of the internal voltage calculated by the transient FEM is different from the trend of the internal voltage when calculated by conventional analytical models at small slot openings. The reason is that analytical models do not consider the influence of leakage flux passing through tooth tips as shown in Fig. 6.

Moreover, leakage flux does not link with windings, so it does not induce voltage in windings.

We now reconsider Fig. 2 that shows that when the slot opening decreases, the mean of the air gap flux density increases. Therefore, if we use the air gap flux density to derive the internal voltage, the voltage amplitude will increase with decreasing slot opening. It can be concluded that if the air gap flux density is used to calculate the internal voltage of the radial-flux PM machine with slotted stator as in conventional analytical models using Carter's theory or in the theory of
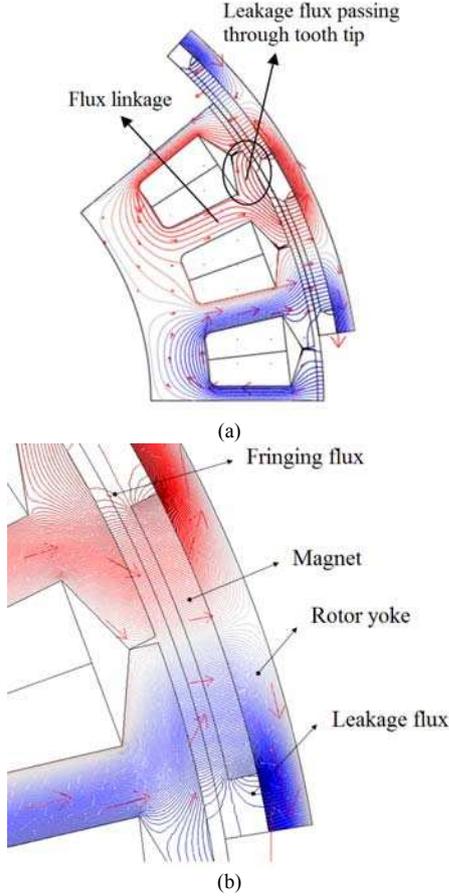

(a)

(b)

Fig. 6. Flux contour of a nearly closed slot. (a) Showing the leakage flux passing through the tooth tip. (b) Showing the fringing flux of a magnet.
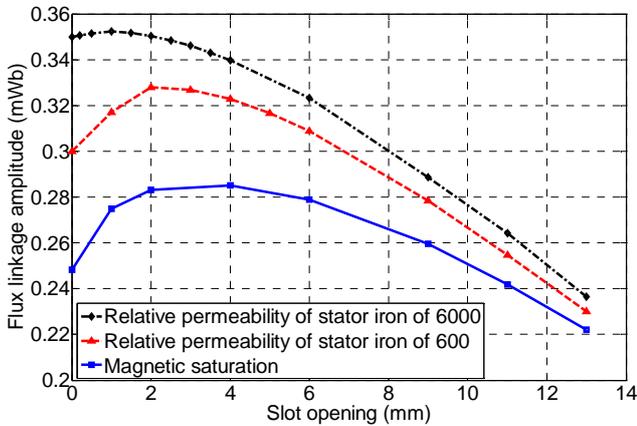

Fig. 7. Influence of the slot opening on the flux linkage amplitude of a turn during no-load.
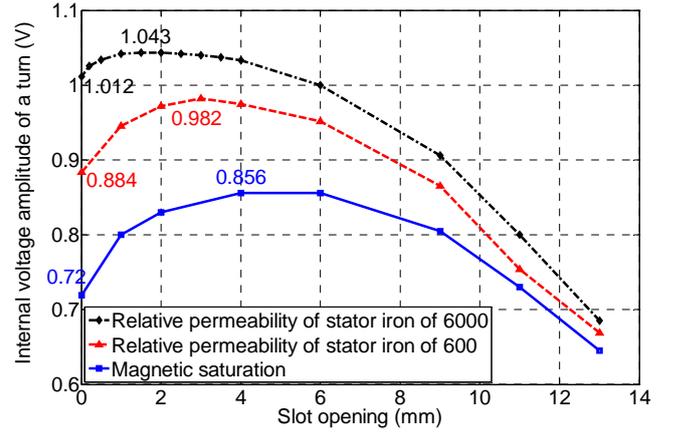

Fig. 8. Influence of the slot opening on the maximum internal voltage of a turn at a speed of 3150 rpm during no-load.

equivalent current sheet placed in air gap, the decrease of the internal voltage at small slot openings cannot be accounted for. This is the limitation of the conventional literature on the slotting effect in the range of small slot opening using the Carter factor and air gap flux density to calculate internal voltage. In fact, the slot opening should be big enough to place the windings into the slots. Analytical design models using Carter factor to account for the slotting effect therefore might be still acceptable for rough design. In Section VII, Carter factor expressions found in literature will be evaluated by comparing them with FEM computations.

V. INFLUENCE OF SLOT OPENING ON MEAN TORQUE

In this section, the influence of the slotting effect on the mean electromagnetic torque of a PM machine is investigated. This torque can be calculated using the Maxwell's stress tensor [22], [23]. In transient 2D-FEM, the equation given below is normally used

$$T = \frac{L}{\mu_0} \oint_l r B_n B_t \, dl \qquad (3)$$

where, B_n and B_t are respectively the normal and tangential components of flux density, μ_0 is the permeability of air, r is the radius, L is the axial length of the stator, and the contour l for calculating the line integral is chosen in the centre of the air gap.

Fig. 9 shows the mean electromagnetic torque versus the slot opening for rated current, at a current angle of 90 degrees, in case of considering magnetic saturation. As can be seen, the slot opening affects mean electromagnetic torque significantly. If slot opening is larger than 4 mm, the flux linkage decreases as shown in Fig. 7 in case of magnetic saturation. Therefore, the mutual torque due to the interaction of the magnetomotive force and the magnetic field of the magnets reduces. Thus, the mean electromagnetic torque decreases when the slot opening increases.

With slot openings smaller than 4 mm, the leakage flux across the tooth tip increases and the flux linkage decreases. Thus, the mean torque also reduces when the slot opening decreases. This has not been described in literature. It has been
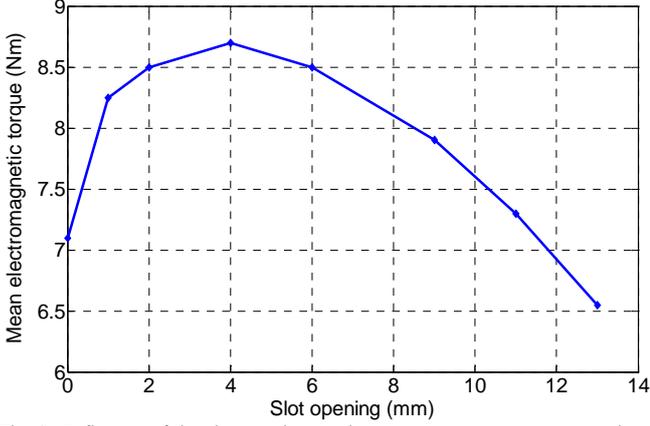
Fig. 9. Influence of the slot opening on the mean torque at a current angle of 90 degrees.

known in literature that when slot opening decreases, air gap flux density increases so that mean electromagnetic torque increases. However, in the range of small slot opening, leakage flux through the tooth tips increases. This causes a decrease of the flux linkage linked by the stator windings and the mean electromagnetic torque. Based on the performance presented in Fig. 9, the slot opening can be selected for maximizing the mean electromagnetic torque. Reconsidering Fig. 8 for the case of magnetic saturation, we see that voltage gets its maximum at the same slot opening as the mean torque.

VI. INFLUENCE OF SLOT OPENING ON IRON LOSSES

To study the influence of the slot opening on the rotor eddy current loss, the electric current in the stator windings is set to zero. Therefore, the rotor eddy current loss is only caused by the slot opening. The rotor eddy current loss due to space harmonic components of magnetomotive force and time harmonic components of the stator current is equal to zero during no-load [25]-[27]. Equations to calculate the stator iron loss are adopted from [24].

A. Rotor Eddy Current Loss Formula

The instantaneous eddy current loss in the rotor can be calculated in 2D transient FEM as

$$P_{edd}(t) = L \iint_S \frac{J_{e,z}^2}{\sigma} dS \tag{4}$$

where, S and L are the cross section area and the length of the conducting region in the z-direction (which is the axial direction of the machine) respectively, $J_{e,z}$ is eddy current in the z-direction, and σ is the electric conductivity, respectively. Note that to satisfy the condition that the eddy current circulates in the magnet, a field-circuit coupled model is applied for each magnet.

B. Magnet Eddy Current Density versus Slot Opening at 3150 rpm

Fig. 10 shows the eddy current density distribution in the middle arc of the magnets. It reaches maximum value at the position opposite slot opening corresponding to an angle of 13 degrees as shown in Fig. 10. The eddy current density in a

fully open slot PM machine is much greater than that in a semi-open slot [26].

The eddy current density in a point in the middle of magnet at a rotor speed of 3150 rpm is depicted in Fig. 11. It is shown that the maximum value of the eddy current density in a point in the middle of the magnet in a fully open slot PM machine is 2.4 times greater than that in a semi-open slot PM machine. As a result, the mean value of the eddy current loss in the fully open slot PM machine is about 5.5 times than that in the semi-open slot PM machine. The magnet eddy current density increases when the slot opening increases. However, the frequency of the eddy current density in a point is not dependent on slot opening. This is because the frequency of the eddy current density is dependent on the number of slots per pole pair and of course on the rotor speed [26]-[27]. The fundamental frequency of the eddy current density f_e is equal to the multiplication of the slot number per pole pair (N_s/p) and the fundamental frequency of the rotating field, $f=(p.n/60)$, where N_s is the number of slots, p is the number of pole pairs and n is the rotational speed of rotor (in rpm). The slot number and the pole number of Machine A are respectively 27 and 18; hence the fundamental frequency of the eddy current in a point is greater than that of the rotating field by a factor of three. The machine has a rated speed of 3150 rpm and the rated fundamental frequency of the rotating
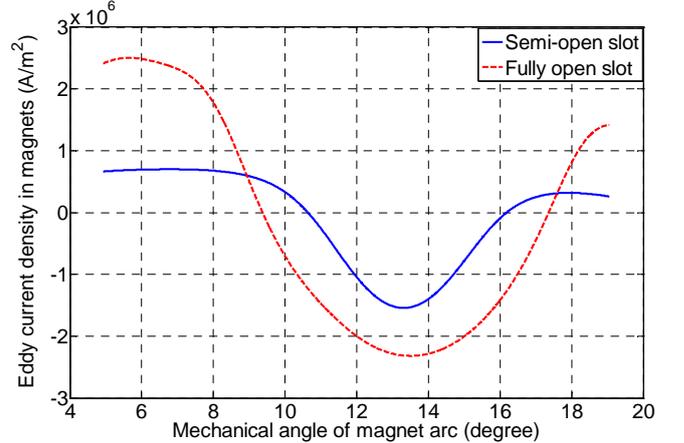

Fig. 10. Eddy current density distribution along arcs in the middle of magnets vs. mechanical angle of the arc at time of 0.1 ms.
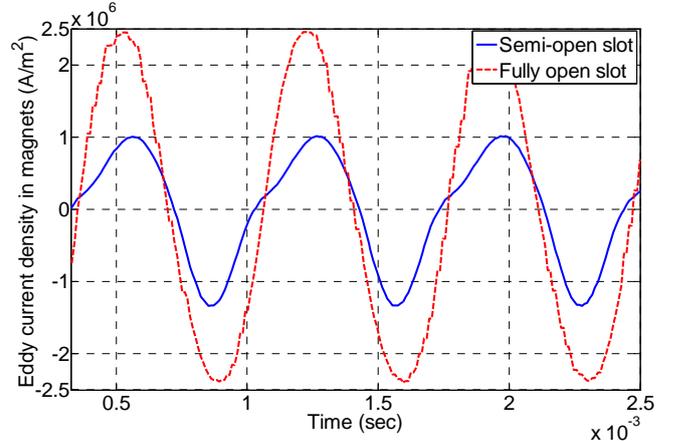

Fig. 11. Eddy current density of points in the middle of magnets vs. time.

field is 472.5 Hz. Hence, the fundamental frequency of the magnet eddy current density at a certain point is 1417.5 Hz. Because of the high frequency, the magnet eddy current loss should be dominant in the total rotor loss. This will be considered in the next subsection.

C. Iron Losses as Function of Slot Opening at 3150 rpm

Fig. 12 shows the eddy current losses in the magnets and the rotor yoke, the total rotor eddy current loss, the stator iron loss, and total iron loss of stator and rotor as a function of the slot opening at the rated speed of 3150 rpm. As can be seen, when the slot opening is smaller than 4 mm, the rotor eddy current losses are negligibly small. With a slot opening greater than 4 mm, the rotor eddy current losses rapidly increase when the slot opening increases. The eddy current loss in the magnets dominates the total eddy current loss in the rotor.

It can be seen that the stator iron loss decreases when the slot opening is greater than 4 mm. This is because the flux linkage decreases as shown in Fig. 7 in case of magnetic saturation. For slot openings between 1 mm and 4 mm, the stator iron loss is nearly constant, because the decrease of the iron losses in the stator teeth and the stator back iron due to the decrease of the flux linkage is compensated by an increase of the iron loss in the tooth tips due to the increase of the leakage flux through the tooth tips. For slot openings between 0 and 1 mm, the decrease of the flux linkage due to the increase of the leakage flux through the tooth tips leads to a decrease of the stator iron loss. For slot openings larger than 7 mm, the rotor eddy current loss is dominant in the total iron loss in stator and rotor. Conversely, when the slot opening is smaller than 7 mm, the stator iron is dominant in the total iron loss.

The total loss increases when the slot opening increases, while the internal voltage (also torque) attains a maximum at a slot opening of 4 mm. If the slot opening is too big or too small, the flux linkage will decrease and the internal voltage will not get its maximum value. Thus, slot opening needs to be designed to compromise between maximizing the internal voltage and minimizing the total loss. With this criterion, the optimal slot opening in Machine A is 4 mm.

From the above analyses, we conclude that if the slot opening is optimized, the internal voltage and the mean torque are maximized, while the total iron loss is minimized.
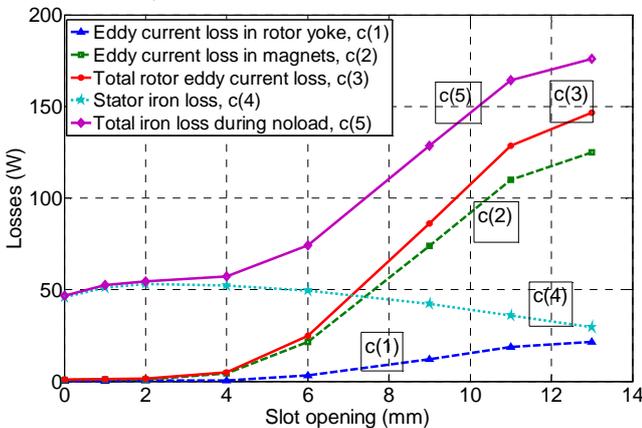

Fig. 12. Losses vs. slot opening at rated speed of 3150 rpm, during no-load.

VII. EVALUATION OF CARTER FACTOR EXPRESSIONS FOUND IN LITERATURE

In Section IV, it was shown that the literature on the slotting effect has limitations for PM machines with small slot openings. When the slot opening is large enough, Carter factor might be used. In this section, Carter's theory of the slotting effect is first reviewed. Then, Carter factor expressions found in literature are evaluated by comparing them with FEM computations.

A. Carter's Theory of Slotting Effect

To include the slotting effect in the analysis and design of electric machines, F.W. Carter proposed to use the effective airgap length g_{eff} instead of the physical air gap length g [3], [4]. This effective length is determined using Carter's factor k_C as

$$g_{eff} = k_C g . \tag{5}$$

The Carter factor k_C is defined as the ratio of the maximum flux density (flux density with zero slot opening) $B_{g,max}$ to the mean flux density $B_{g,0}$ in air gap at regions opposite to a magnet [4], [22]. It can be expressed as,

$$k_C = \frac{B_{g,max}}{B_{g,0}} = \frac{g_{eff}}{g} = \frac{\tau_s}{\tau_s - \gamma g} \tag{6}$$

where, g is the physical air gap length, g_{eff} is the effective air gap, and τ_s is the slot pitch, respectively. Curve (1) in Fig. 13 illustrates the air gap flux density including slotting effect, but excluding fringing. While curve (2) is equivalent to the air gap flux density for the traditional analytical design model.

The following expressions of the factor γ have been proposed to calculate the Carter factor:

$$\gamma = \frac{(b_s / g)^2}{5 + (b_s / g)} \tag{7}$$

$$\gamma = \frac{(b_s / g)^2}{4.4 + 0.75(b_s / g)} \tag{8}$$

$$\gamma = \frac{4}{\pi} \left[\frac{b_s}{2g} \arctan\left(\frac{b_s}{2g}\right) - \ln\sqrt{1 + \left(\frac{b_s}{2g}\right)^2} \right] \tag{9}$$

$$\gamma = \frac{2b_s}{\pi g} \left[\arctan\left(\frac{b_s}{2(l_m + g)}\right) - ... \\ ... - \frac{(l_m + g)}{b_s} \ln\sqrt{1 + \left(\frac{b_s}{2(l_m + g)}\right)^2} \right] \tag{10}$$

$$\gamma = \frac{\tau_s}{g} \left\{ \frac{b_s}{\tau_s} - \frac{4g}{\pi\tau_s} \ln(1 + \frac{\pi b_s}{4g}) \right\} \tag{11}$$

where, l_m is the length of magnet and b_s is the slot opening.

Equations (7)-(9) were derived for the wound field machines, but they are used for PM machines in current literature on analytical design [7]. Equations (7) and (8) can be found in [7], [28], while (9) was given by Carter in [4]. Equation (10) is given by [29] for PM machines, while (11)

can be found in [7], [8]. Almost all the equations above have been derived using conformal transformations. Equation (11) has been derived using analytical calculations. It can be seen from the above equations that the Carter factor increases when g/τ_s decreases and/or when b_s/τ_s increases.

These expressions will be evaluated by comparing them with results calculated by FEM in the next subsection to find the most suitable one for the design of PM machines.
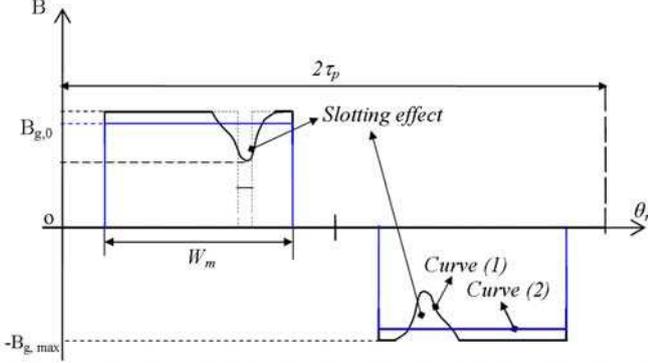

Fig. 13. Illustration of air gap flux density during no-load, excluding the fringing effect of magnet, where τ_p and W_m denote the pole pitch and the pole width, respectively.

B. Evaluation of Carter Factor Expressions

In conventional analytical design models of slotted PM machines, the Carter factor is important. This factor influences the calculation results of air gap flux density, voltage, etc. The electromagnetic force, torque, and voltage are calculated based on the magnetic field in the air gap. Thus, if the air gap flux density calculation is improved, the analytical model accuracy will also be improved. The Carter factor expressions are evaluated by comparing the results to FEM computations to find the most suitable expression for the design and analysis of PM machines considered in this study.

For clarity, we define three correction factors. First, the FEM slotting factor or FEM Carter factor is a factor accounting for the slotting effect and calculated by a static FEM computation at a single rotor position. Second, the FEM fringing factor is a factor accounting for the fringing flux of the magnets (as shown in Fig. 6b) and calculated by a static FEM computation at a single rotor position for a closed slot PM machine. Third, the correction factor calculated by a static FEM including both the slotting and fringing effects is called total FEM correction factor.

For the sake of comparison of the Carter factor expressions and the FEM Carter factor, we have to separate the slotting and the fringing effect of the magnets in the FEM calculation as follows.

First, it is necessary to explain the fringing phenomenon. The fringing effect of a magnet is a field phenomenon, in which the corners in the air gap flux density waveform due to the magnet become rounded and the flat top becomes narrower as shown by curve (1) in Fig. 14. Curve (1) is the air gap flux density including the fringing effect with zero slot opening, calculated by static FEM. Curve (2) is the air gap flux density calculated with an analytical method neglecting the fringing effect. Curve (3) is the mean flux density of points opposite to the magnets, derived from curve (1). The fringing effect causes the decrease of mean of air gap flux density per pole as well as of the internal voltage. However, the fringing effect reduces the amplitude of the harmonic components making the air gap flux density and the voltage more sinusoidal.

Similar to the slotting effect, the fringing effect can be taken into account by using the fringing correction factor. When the slot opening is equal to zero, slotting factor is equal to one, so the fringing factor can be calculated by a FEM computation for this case. The FEM fringing factor is calculated according to (6), in which the air gap flux density is calculated by a static FEM computation for the PM machine with zero slot opening. The resulting FEM fringing factor has a value of 1.06. The FEM fringing factor mainly depends on the air gap length and the dimensions of the magnet. The FEM slotting factor (or FEM Carter factor, curve (7) in Fig. 15) is therefore equal to the total FEM factor (curve (6) in Fig. 15) minus the FEM fringing factor of 1.06 plus 1. The relationship of correction factors can be expressed as [4], [18]

$$k_{tol} = k_C + k_{fringing} - 1 \tag{12}$$

where k_{tol} is the total FEM correction factor accounting for both the slotting effect and the fringing effect, k_C is the FEM Carter factor, and $k_{fringing}$ is the FEM fringing factor.

Fig. 15 shows the correction factors versus the slot opening. Curves (1) to curve (5) are respectively calculated corresponding to equations (7) to (11). The total FEM correction factor including the slotting effect and the fringing effect is curve (6). It is calculated according to (6) by the static FEM. In the analytical equations of the Carter factor, the fringing effect of the magnets is not included. Therefore, when the slot opening reaches zero, the Carter factor approaches the value of one. However, the fringing effect of the magnets is included in the FEM calculation, so that curve (6) is greater than one, even when the slot opening reaches to zero. Note that the radial flux density is calculated at the arc in the middle of the air gap so that the edge effect of the slot opening can be neglected as can be seen in Fig. 2 and Fig. 3.

It can be seen in Fig. 15 that the analytical Carter factor--curves (1), (3), (4) and FEM Carter factor--curve (7) have a similar trend, but the value is significantly different. Curves (1) and (3) are almost the same. Curves (2) and (7) match for slot openings smaller than 9 mm, otherwise their discrepancy increases when the slot opening increases. Curves (5) and (7) match, but the trend is a bit different when the slot opening is over 12 mm. In summary, curve (5) is the closest to the FEM Carter factor. The fringing effect is significant, so it is recommended to be considered in design of PM machines.

The method to calculate correction factors based on the static FEM at a single rotor position in this section can be used for a hybrid model that combines the analytical model and the static FEM model for improving the accuracy of the traditional Analytical design model [18]. However, hybrid model is beyond the scope of this paper.
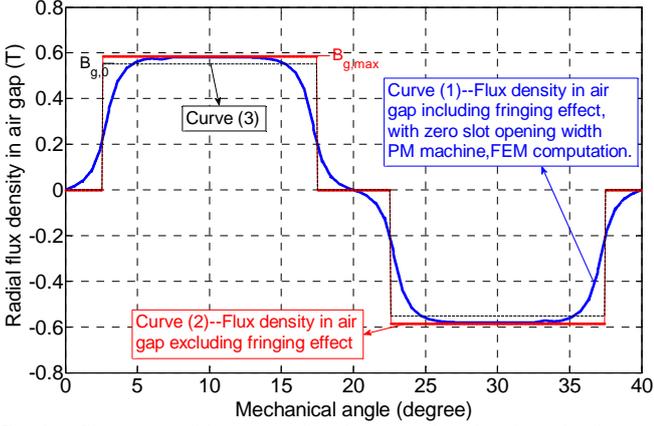
Fig. 14. Illustration of the air gap flux density with and without the fringing effect of magnets, excluding the slotting effect.
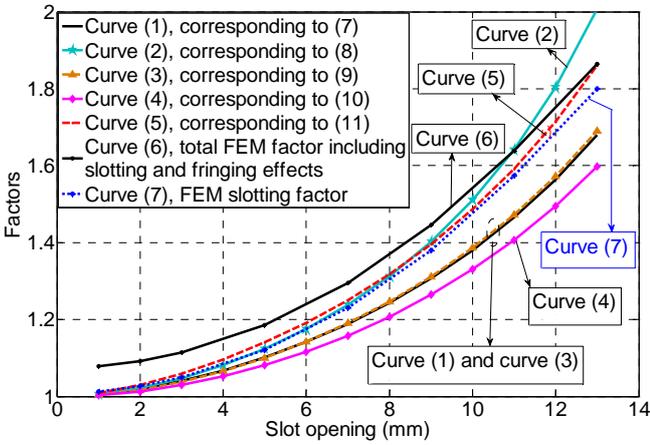

Fig. 15. Comparison of the Carter factor calculated by FEM and analytical expressions.

VIII. MEASUREMENT AND VALIDATION

A. Experimental Validation of Flux Linkage and Internal Voltage

To measure the internal voltage of a turn and the flux linkage of the PM machine A with semi-open slots, a turn is wound around a tooth. We measured the voltage at the terminals of the turn at a rotor speed of 2347 rpm. A comparison of simulation and experimental results of the flux linkage and the internal voltage are presented in Fig. 16. The flux linkage and internal voltage are respectively calculated according to (1) and (2) by the transient FEM program. The measured flux linkage is obtained by integrating the measured internal voltage of the turn with respect to time. Fig. 16 shows that there is a good agreement between measured and simulated amplitudes and waveforms. The discrepancy between the measured and simulated internal voltage amplitude is about 3.5%.

Fig. 17 compares the phase internal voltage simulation and experiment. The FEM simulation and the experiment are in good agreement with a maximum error in the internal voltage amplitude of about 4% for the range of rotor speed from 300 rpm to 3150 rpm.

B. Additional Experimental Validation of Slotting Effect on Internal Voltage

In the previous subsection, the computation of the flux linkage and the internal voltage of machine A was validated. In this subsection, the internal voltage computation is additionally validated for PM machines with semi-open (machine B) and fully open slots (machine C) shown in Fig. 18.

Fig. 19a and Fig. 19b respectively show FEM simulations of the surface flux density of machine B and machine C. It can be seen that in the same rotor position, the maximum flux density in a tooth of machine B (being 1.75 T) is higher than that of the fully open slot machine C (being 1.61 T). It means that the amplitude of the flux linkage of a coil around a tooth as well as the internal voltage of a turn in the former is higher than that in the latter. Internal voltage comparison of simulation and experimental results for the semi-open slot machine B and the fully open slot machine C shown in Fig. 20a and Fig. 20b are in good agreement. It is confirmed that the nonlinear transient 2D-FEM model including rotor motion is accurate and suitable for analysis and design of PM machines in the application considered in this paper.
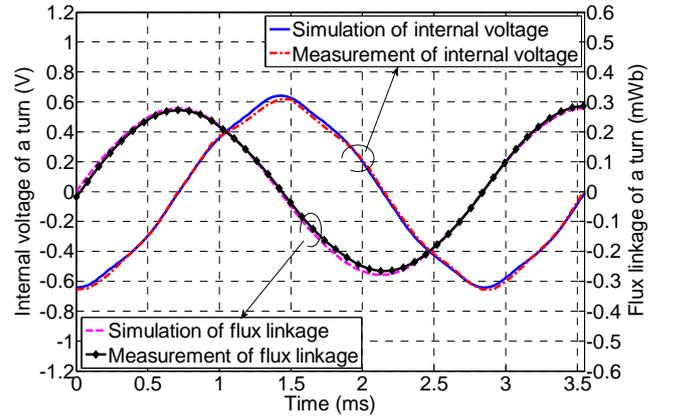

Fig. 16. Comparison between simulation and experimental results in two cases: internal voltage of a turn and flux linkage of a turn, using machine A.
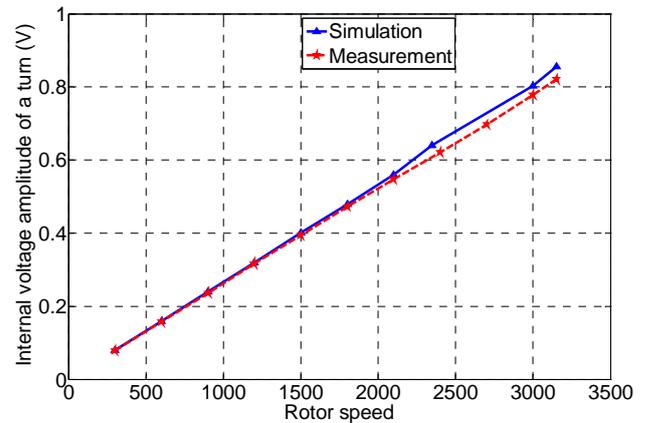

Fig. 17. Comparison of the simulated and measured internal voltage of machine A.
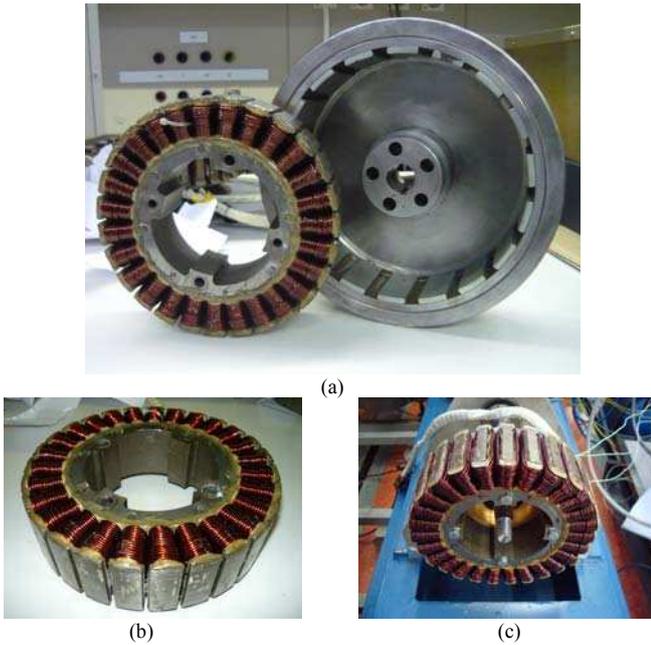
(a)

(b)

Fig. 20. Internal voltage vs. rotor speed, comparison of simulation and experimental results. (a) Machine B with semi-open slot. (b) Machine C with fully open slot.

IX. CONCLUSION

In this paper, the influence of the slot opening on the distribution of the flux, the flux linkage, the internal voltage, the torque and the eddy current loss is investigated. It was found that for small slot openings, the flux linkage, internal voltage, and torque computed using transient FEM simulations including rotor motion do not increase with decreasing slot opening as predicted by conventional analytical models based upon the Carter factor. They in fact decrease. These FEM computations were validated using measurements on three permanent magnet machines with different slot openings. The measured and simulated values for the flux linkage and the internal voltages were shown to match very well. Our study yields valuable insight in the optimization of the slot opening in order to maximize the internal voltage and torque.

REFERENCES

[1] Holm, S.R.; Polinder, H.; Ferreira, J.A.; , "Analytical Modeling of a Permanent-Magnet Synchronous Machine in a Flywheel," *Magnetics, IEEE Transactions on* , vol.43, no.5, pp.1955-1967, May 2007.

[2] EL-Refaie, A.M.;, "Fractional-Slot Concentrated-Windings Synchronous Permanent Magnet Machines: Opportunities and Challenges*," Industrial Electronics, IEEE Transactions on* , vol.57, no.1, pp.107-121, Jan. 2010.

[3] Carter, F.W.; , "Note on air-gap and interpolar induction," *Electrical Engineers, Journal of the Institution of* , vol.29, no.146, pp.925-933, July 1900.

[4] Carter, F.W.; , "The magnetic field of the dynamo-electric machine," *Electrical Engineers, Journal of the Institution of* , vol.64, no.359, pp.1115-1138, November 1926.

[5] Zarko, D.; Ban, D.; Lipo, T.A.; , "Analytical calculation of magnetic field distribution in the slotted air gap of a surface permanent-magnet motor using complex relative air-gap permeance," *Magnetics, IEEE Transactions on* , vol.42, no.7, pp. 1828- 1837, July 2006.

[6] Boughrara, K.; Ibtiouen, R.; Žarko, D.; Touhami, O.; Rezzoug, A.; , "Magnetic Field Analysis of External Rotor Permanent-Magnet Synchronous Motors Using Conformal Mapping," *Magnetics, IEEE Transactions on* , vol.46, no.9, pp.3684-3693, Sept. 2010.

[7] Duane, C.H.; "Brushless Permanent Magnet Motor Design"; McGraw-Hill, New York, 1994.

[8] Lipo, T.A.; "Introduction to AC Machine Design", Wisconsin Power Electronics Research Center, Univ. Wisconsin, Madison, 1996.

(a)

Fig. 18. (a) An exterior rotor PM machine with concentrated windings, 27slots/18poles in a flywheel. (b) Stator with semi-open slot, slots opening of 4 mm. (c) Stator with fully open slot, slots opening of 13 mm.
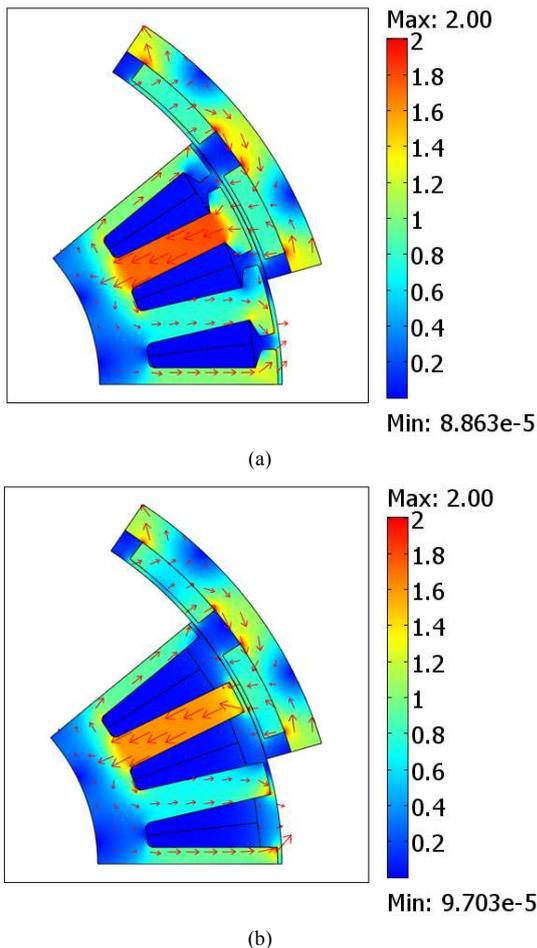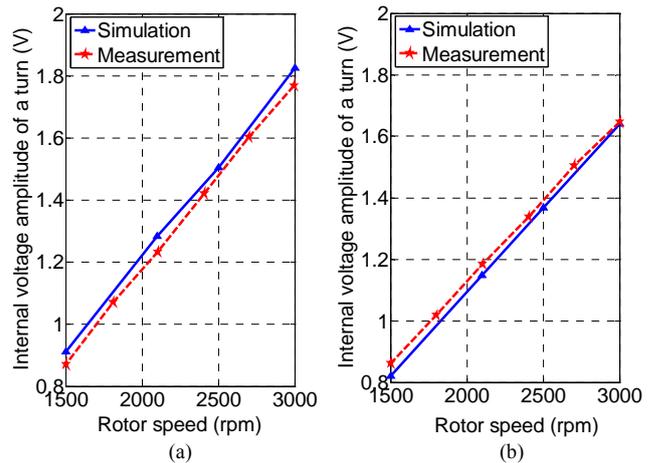

(a)

(b)

Fig. 19. Nonlinear transient FEM simulation including rotor motion for machines B and C; surface and arrow are magnetic flux density (T). (a) Semi-open slot. (b) Fully open slot.

[9] Zhu, Z.Q.; Howe, D.; Bolte, E.; Ackermann, B.; , "Instantaneous magnetic field distribution in brushless permanent magnet DC motors. I. Open-circuit field," *Magnetics, IEEE Transactions on* , vol.29, no.1, pp.124-135, Jan 1993.

[10] Gerling, D.; , "Influence of the stator slot opening on the characteristics of windings with concentrated coils," *Electric Machines and Drives Conference, 2009. IEMDC '09. IEEE International* , vol., no., pp.1710-1714, 3-6 May 2009.

[11] Dajaku, G.; Gerling, D.; , "Stator Slotting Effect on the Magnetic Field Distribution of Salient Pole Synchronous Permanent-Magnet Machines," *Magnetics, IEEE Transactions on* , vol.46, no.9, pp.3676-3683, Sept. 2010.

[12] Chen, J.T.; Zhu, Z.Q.; Iwasaki, S.; Deodhar, R.P.; , "Influence of Slot Opening on Optimal Stator and Rotor Pole Combination and Electromagnetic Performance of Switched-Flux PM Brushless AC Machines," *Industry Applications, IEEE Transactions on* , vol.47, no.4, pp.1681-1691, July-Aug. 2011.

[13] Wu, L.J.; Zhu, Z.Q.; Staton, D.; Popescu, M.; Hawkins, D.; , "Subdomain Model for Predicting Armature Reaction Field of Surface-Mounted Permanent-Magnet Machines Accounting for Tooth-Tips," *Magnetics, IEEE Transactions on* , vol.47, no.4, pp.812-822, April 2011.

[14] Wu, L.J.; Zhu, Z.Q.; Staton, D.; Popescu, M.; Hawkins, D.; , "An Improved Subdomain Model for Predicting Magnetic Field of Surface-Mounted Permanent Magnet Machines Accounting for Tooth-Tips," *Magnetics, IEEE Transactions on* , vol.47, no.6, pp.1693-1704, June 2011.

[15] Zhu, Z.Q.; Wu, L.J.; Xia, Z.P.; , "An Accurate Subdomain Model for Magnetic Field Computation in Slotted Surface-Mounted Permanent-Magnet Machines," *Magnetics, IEEE Transactions on* , vol.46, no.4, pp.1100-1115, April 2010.

[16] Lubin, T.; Mezani, S.; Rezzoug, A.; , "Exact Analytical Method for Magnetic Field Computation in the Air Gap of Cylindrical Electrical Machines Considering Slotting Effects," *Magnetics, IEEE Transactions on*, vol.46, no.4, pp.1092-1099, April 2010.

[17] Linni Jian; Guoqing Xu; Mi, C.C.; Chau, K.T.; Chan, C.C.; , "Analytical Method for Magnetic Field Calculation in a Low-Speed Permanent-Magnet Harmonic Machine," *Energy Conversion, IEEE Transactions on*, vol.26, no.3, pp.862-870, Sept. 2011.

[18] VuXuan, H.; Lahaye, D.; Polinder, H.; Ferreira, J.A.; , "Improved model for design of permanent magnet machines with concentrated windings," *Electric Machines & Drives Conference (IEMDC), 2011 IEEE International* , vol., no., pp.948-954, 15-18 May 2011.

[19] Xuan, H.V.; Ani, S.O.; Lahaye, D.; Polinder, H.; Ferreira, J.A.;, "Validation of non-linear dynamic FEM model for design of PM machines with concentrated windings in ship application," *Power Electronics and Applications (EPE 2011), Proceedings of the 2011-14th European Conference on* , vol.1, no., pp.1-9, Aug. 30 2011-Sept. 2011.

[20] Hung Vu Xuan; Lahaye, D.; Hoeijmakers, M.J.; Polinder, H.; Ferreira, J.A.; , "Modeling magnetic saturation for the design of exterior rotor permanent magnet machines*," Power Electronics Conference (IPEC), 2010 International* , vol., no., pp.1299-1305, 21-24 June 2010.

[21] Jabbar, M.A.; Hla Nu Phyu; Zhejie Liu; Chao Bi; , "Modeling and numerical simulation of a brushless permanent-magnet DC motor in dynamic conditions by time-stepping technique," *Industry Applications, IEEE Transactions on* , vol.40, no.3, pp. 763- 770, May-June 2004.

[22] Pyrhonen, J.; et al, "Design of Rotating Electrical Machines", John Wiley& Sons, Ltd, 2008.

[23] Bianchi, N.; Bolognani, S.; , "Design techniques for reducing the cogging torque in surface-mounted PM motors," *Industry Applications Conference, 2000. Conference Record of the 2000 IEEE* , vol.1, no., pp.179-185 vol.1, 2000.

[24] VuXuan, H.; Lahaye, D.; Ani, S.O.; Polinder, H.; Ferreira, J.A.; , "Electrical generators for maritime application," *Electrical Machines and Systems (ICEMS), 2011 International Conference on* , vol., no., pp.1-6, 20-23 Aug. 2011.

[25] Yamazaki, K.; Fukushima, Y.; , "Effect of Eddy-Current Loss Reduction by Magnet Segmentation in Synchronous Motors With Concentrated Windings," *Industry Applications, IEEE Transactions on* , vol.47, no.2, pp.779-788, March-April 2011.

[26] Hung Vu Xuan; Lahaye, D.; Hoeijmakers, M.J.; Polinder, H.; Ferreira, J.A.; , "Studying rotor eddy current loss of PM machines using nonlinear FEM including rotor motion," *Electrical Machines (ICEM), 2010 XIX International Conference on* , vol., no., pp.1-7, 6-8 Sept. 2010.

[27] Amara, Y.; Jiabin Wang; Howe, D.; , "Analytical prediction of eddy-current loss in modular tubular permanent-magnet machines," *Energy Conversion, IEEE Transactions on* , vol.20, no.4, pp. 761- 770, Dec. 2005.

[28] Nasar, S.A.; , "Electromagnetic theory of electrical machines," *Electrical Engineers, Proceedings of the Institution of* , vol.111, no.6, pp.1123-1131, June 1964.

[29] Qishan, G.; HongZhan, G.; "Effective Slotting in Permanent Magnet Electric Machines"; *Electric Machines and Power Systems,* 1985.